Journal of Hazardous Materials 175 (2010) 715–725

Contents lists available at ScienceDirect

Journal of Hazardous Materials

journal homepage: www.elsevier.com/locate/jhazmat

Preparation of capsules containing 1-nonanol for rapidly removing high concentration phenol from aqueous solution

Guanghui Zhao, Yanfeng Li*, Xiaoxia Liu, Xiaoli Liu

State Key Laboratory of Applied Organic Chemistry, College of Chemistry and Chemical Engineering, Institute of Biochemical Engineering & Environmental Technology, Lanzhou University, 222 Tianshui Road, Lanzhou 730000, China

ARTICLE INFO

Article history:
Received 25 June 2009
Received in revised form 16 October 2009
Accepted 16 October 2009
Available online 27 October 2009

Keywords:
Adsorption
Phenol
Polysulfone
1-Nonanol
Capsule

ABSTRACT

This study investigated the potential of capsules containing 1-nonanol for the adsorption of phenol at high initial concentrations. The polysulfone capsules containing 1-nonanol (PSF@1-nonanol capsules) were successfully prepared with a phase inversion method, and the results showed that 1-nonanol was encapsulated with polysulfone as an encapsulation capacity of 67.99% was achieved. Systematic studies on phenol adsorption equilibrium, kinetics and isotherms by PSF@1-nonanol capsules were carried out. The results showed that the rate of adsorption of phenol is initially quite rapid and equilibrium is reached in about 90 min. Phenol adsorption uptake was found to increase with increase in initial concentration and adsorption time, whereas adsorption of phenol was more favourable at acidic pH and low temperature. The adsorption kinetics of phenol followed pseudo-second-order model, and the best fits of adsorption isotherms were achieved with the Freundlich equation. These results demonstrate that the use of PSF@1-nonanol capsules enhanced the mass transfer rate and the uptakes to phenol at high initial concentrations. Furthermore, after seven times of repeated extraction and stripping, the microcapsules kept almost the same adsorption ability, which indicated that the PSF@1-nonanol capsules have very good stability in the adsorption process. Therefore, PSF@1-nonanol capsules can be taken as an ideal adsorbent for rapid removal of high concentration phenol from aqueous solution.

1. Introduction

Phenol is a toxic and mutagenic substance at high concentrations and may be absorbed through the respiratory organ, skin, and the alimentary canal [1,2]. The ingestion of such contaminated water in the human body causes protein degeneration, tissue erosion and paralysis of the central nervous system and also damages the kidney, liver and pancreas [3]. Based on severe chronic toxicity, phenol has been classified as a high concern priority pollutant by the EPA [4]. Therefore, the treatment of high concentration phenol effluent is considered necessary.

Conventional methods for the removal of phenol in effluents include physical, chemical, and biological processes [5]. Physical adsorption is generally considered to be an effective method for quickly lowering the concentration of dissolved phenol in an effluent. A considerable amount of work has also been reported in the literatures regarding the adsorption of phenol on various solid phase adsorbent surfaces such as activated carbon [6–8], natural materials [9,10], bioadsorbents [11–13], waste materials [14–16], and so on. However, most of them present some limitations such as poor regeneration capacity or slow absorption rate. On the contrary, liquid–liquid extraction presents a rapid absorption rate, but liquid phase extraction is easy to form an emulsion or a third phase in the extraction process, which causes the extractant loss and damage to water resource. More importantly though, the use of large amounts of toxic organic solvents poses a health hazard to personnel and results in the production of hazardous waste, thus adding extra operational costs for waste treatment. In order to overcome these drawbacks, the extractant liquid phase could be immobilized into the porous structure or cavities of the support through encapsulation [17]. Compared to conventional liquid–liquid extraction, there are several advantages with solvent capsules as separation agent, such as good stability, high selectivity, minimal use of organic solvents and easy phase separation [18]. However, most of the applications focus on the recovery of heavy metals and immobilization of ionic liquid [19–29].

To our knowledge, the encapsulation of a specific extractant of an organic pollutant from water samples has uncommonly been investigated. Therefore, the aim of the present study was to investigate the sorption behavior of phenol from high concentration phenol solution with 1-nonanol impregnated capsules (1-nonanol is an effective compound to remove phenol from aqueous solution [30]). The capsules were synthesized by phase inversion (immersion) precipitation technique, using polysulfone (PSF) as

* Corresponding author. Tel.: +86 931 8912528; fax: +86 931 8912113.
E-mail address: liyf@lzu.edu.cn (Y. Li).

0304-3894/$ – see front matter © 2009 Elsevier B.V. All rights reserved.
doi:10.1016/j.jhazmat.2009.10.068

a shell material, N-methyl-2-pyrrolidinone (NMP) as solvent, and 1-nonanol as the core. The sorption behavior will be discussed according to kinetic and isotherm models. The stability of the capsules has been investigated too.

2. Materials and methods

2.1. Chemicals and reagents

Phenol (99.5%, assay) was purchased from Tianjin Guangfu Fine Chemical Research Institute (China). 1-Nonanol was purchased from Beijing Chemical Reagent Corporation. Polysulfone (PSF) with intrinsic viscosity of 0.56 was purchased from DaLian Polysulfone Plastic CO. LTD. (China). All the other materials were obtained from Tianjin Guangfu Fine Chemical Research Institute (China), used as received without any further purification.

2.2. Preparation of PSF@1-nonanol capsules

PSF@1-nonanol capsules were prepared as follows: 8 g of PSF was dissolved in 60 mL of N-methyl-2-pyrrolidinone (NMP) to obtain the PSF solution. Then 24 g of 1-nonanol (the mass ratios of PSF to 1-nonanol was 1:3) was added into the solution of PSF and stirred for 60 min under the room temperature, and the dispersed phase of 1-nonanol and PSF was obtained. The dispersed phase of 1-nonanol and PSF was injected into the solidification solution (0.5 wt.% sodium dodecylbenzenesulfonate in aqueous solution) using a 1.2-mm diameter syringe needle to obtain PSF@1-nonanol capsules. Then, they were washed with deionized water several times and kept in deionized water for the extraction process; finally, PSF@1-nonanol capsules were air-dried at room temperature. Due to the difficulty to prepare particles of regular shape when the proportion of 1-nonanol is higher than 75% in the capsules, the proportion was deemed as the highest proportion for the preparation process. In this study, the mass ratios of PSF to 1-nonanol were controlled at 1:0, 1:1 and 1:3. The PSF@1-nonanol capsules used in this study is the capsules whose mass ratio of PSF to 1-nonanol was controlled at 1:3, except for special clarification. The obtained PSF@1-nonanol capsules were characterized by means of scanning electron microscopy (SEM, JSM-6380Lv, JEOL, Japan; and JSM-6701F, JEOL, Japan) and optical microscope (SMZ-168, Motic, China). The encapsulation capacity of 1-nonanol was measured by thermogravimetric analyzer (TGA, STA449, Netzsch, Germany). The Brunauer–Emmett–Teller (BET) surface area of PSF@1-nonanol capsules was obtained from N_2 adsorption isotherms at 77 K with a Micromeritics' ASAP 2020 (Accelerated Surface Area and Porosimetry) analyzer.

2.3. Adsorption experiments

The experiment was carried out in a batch reactor, which was put into a temperature controlled water bath. 6 g of PSF@1-nonanol capsules were added into each of six 125 mL Erlenmeyer flasks containing 70 mL of phenol solution. The flasks were sealed with rubber stoppers, agitated at 180 rpm. The adsorption of the phenol was calculated by the difference in their initial and final concentrations. Effect of pH (2–12), contact time (5–120 min), initial phenol concentration (1000–10,000 mg/L) and temperature (20, 40 and 60 °C) was studied. Each experiment was repeated three times and the given results were the average values. The variation of the uptake of phenol with adsorption time was investigated in kinetic experiments.

Phenol concentration in the supernatant solution was estimated colorimetrically according to the method previously described by Yang and Humphrey [31] based on rapid condensation with 4-aminoantipyrene followed by oxidation with alkaline potassium ferricyanide and the absorbancy read at 510 nm. The amount of phenol adsorbed onto the PSF@1-nonanol capsules was calculated from the mass balance of the equation as given below:

$$Q_e = (C_0 - C_e)\frac{V}{W} \quad (1)$$

The percentage of phenol removed (R%) from the solution was calculated using the following equation:

$$R\ (\%) = \frac{C_0 - C_e}{C_0} \times 100 \quad (2)$$

where C_0 and C_e are the initial and equilibrium concentration of phenol solution (mg/L), respectively, Q_e is equilibrium adsorption capacity of phenol on PSF@1-nonanol capsules (mg/g), V is the volume of the phenol solution (L) and W is the mass of the PSF@1-nonanol capsules used (g).

2.4. Regeneration of the capsules

After batch sorption, we resuspended the wet phenol-laden capsules from the sorption experiment in 15 mL of sodium hydroxide solution (0.5 M). The suspension was subsequently equilibrated for 60 min at 20 °C with shaking at 180 rpm. The capsules were then washed with deionized water to pH 6.0. Phenol adsorption experiments were re-conducted at 20 °C to evaluate the new adsorption capacity of phenol onto the regenerated PSF@1-nonanol capsules from aqueous solutions. Multiple column adsorption–regeneration cycles of PSF@1-nonanol capsules were also performed to further test its potential application. 1.0 g of the PSF@1-nonanol capsules were packed into a glass column (1.0 cm in diameter and 20 cm in height), which was put into a constant temperature incubator and maintained at 20 °C. A phenol concentration of approximately 1822 mg/L was used, and the pH of the phenol solutions applied to the column was 6.0. The phenol solutions were fed by a peristaltic pump through the column at 1.0 mL/min. After the column reached exhaustion, i.e. when the ratio of effluent to influent concentration exceeded a value of 0.9 or higher, the column saturated with phenol was eluted using 0.5 M sodium hydroxide solution (50 mL) to desorb phenol from the capsules. After elution, deionized water was used to rinse/regenerate the capsules until the pH in the wash effluent reached 6.0. Then, the column was fed again with phenol solution for the new cycle of operation to investigate the potential of reusing the capsules for phenol adsorption.

3. Results and discussion

3.1. Preparation of PSF@1-nonanol capsules

A liquid–liquid phase separation technique was employed to fabricate the PSF@1-nonanol capsules (Fig. 1). Figs. 2 and 3 demonstrate that the structure of the capsules is similar to that of erythrocytes and there are many regular wrinkles on the external surface. The growing process of PSF@1-nonanol capsules is described as follows (Fig. 1): when the PSF/1-nonanol solution drop contacts with the solidification solution (0.5 wt.% sodium dodecylbenzenesulfonate in aqueous solution), the rapid exchange of the solvent NMP and water occurred, at the same time, the influx of water was small, a skin layer formed due to the rapid phase separation (Fig. 3(d)), and many pores existed in the capsules, which can be found in Fig. 3(c). Smolders and coworkers [32] suggested the large pore in the center (Fig. 3(d)) was formed by anomalous growth of nuclei. With the completion of the exchange between NMP and water, the porous PSF@1-nonanol capsules were prepared (Fig. 3(a) and (b)). Fig. 3(a) clearly shows the biconcave disc-shaped structure of the prepared capsules, which have an average diameter of 2–2.5 mm with sufficient rigidity. However, capsules

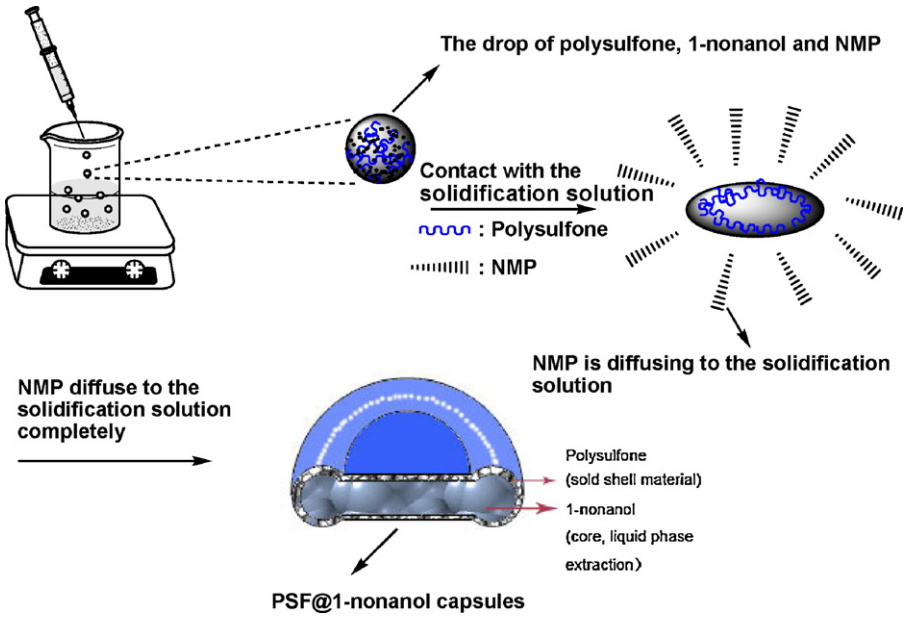

Fig. 1. Scheme for the preparation of PSF@1-nonanol capsules.

containing extractant prepared by previous researchers are all spherical [19–29]. Compared to spherical capsules, the biconcave disc-shaped capsules present a larger contact surface between the extractant and the inner surface of the capsules, which benefits mass transfer performance. In Fig. 3(b), the regular wrinkle was found on the outer surface of the capsule. Compared to the smooth surface, the wrinkle enlarges surface area, which also benefits mass transfer performance. Therefore, its characteristic biconcave disc-shaped and rugate morphology suggests that phenol from aqueous solution should be removed rapidly by PSF@1-nonanol capsules.

Fig. 4 shows SEM images of cross-section of extractant-loaded capsules and de-extractant capsules, which show great difference between the capsules. The de-extractant capsules were prepared according to Ref. [18]. Two grams of PSF@1-nonanol capsules were put into 100 mL ethanol for 48 h under stirring. Then the capsules were taken out and dried. As Ref. [18] described, there are a lot of small spheres (1-nonanol clusters) with a diameter of several microns in the wall of the extractant-loaded capsules, as shown in Fig. 4(a). But for the de-extractant capsules only supported porous structure formed by PSF (shell) can be seen from Fig. 4(b). The difference indicates that 1-nonanol was successfully encapsulated in small sphere form.

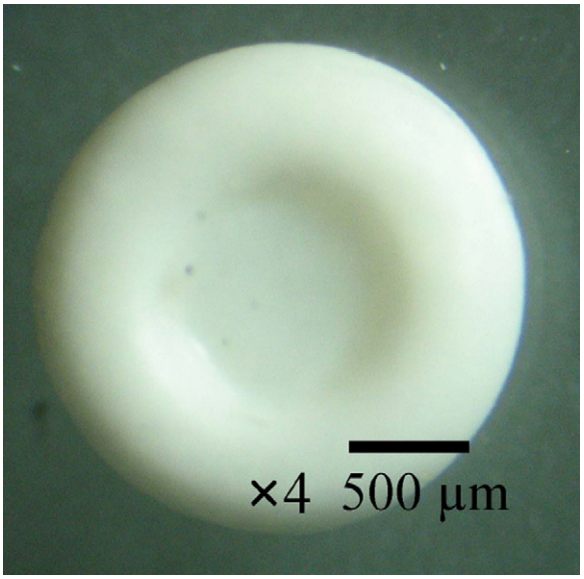

Fig. 2. The optical microscope photographs of PSF@1-nonanol capsules.

The surface area and porosity data are summarized in Table 1. It was noticed that de-extractant capsules possess much higher surface area and much more porous volume than extractant-loaded capsules. This phenomenon can be further explained by understanding the characters of PSF@1-nonanol capsules used in this study. The encapsulated 1-nonanol molecules will be associated with each other to form 1-nonanol clusters (as shown in Fig. 4(a)), which are remarkably stabilized in pores of PSF@1-nonanol capsules, causing partial blockage of the pores, reducing the accessible surface area and porous volume. De-extractant capsules and extractant-loaded capsules will be used to adsorb phenol, respectively, in the following research to further understand the above phenomenon.

In order to observe the encapsulation capacity of PSF@1-nonanol capsules, thermogravimetric analysis (TGA) of capsules was carried out. TGA was conducted with a TA Instruments STA449, and experiments were carried out on approximately 10 mg of samples in flowing air (flowing rate = 100 cm^3/min) at a heating rate of 20 °C/min. Fig. 5 shows the TGA result of PSF@1-nonanol capsules, which began to decompose at 100.54 °C, while PSF began to decompose at 483.04 °C. The encapsulation capacity of capsules as calculated was 67.99%, which was much better than other works [17,29].

3.2. Adsorption studies

3.2.1. The contribution of 1-nonanol and PSF for phenol adsorption

The PSF@1-nonanol capsules include PSF and 1-nonanol, in order to investigate the adsorption capacity contribution of them, PSF@1-nonanol capsules of the different mass ratios (PSF to 1-nonanol) were prepared and used to adsorb phenol, respectively. In this study, the mass ratios of PSF to 1-nonanol were controlled at 1:0, 1:1 and 1:3, and these capsules were coded as PSF, PSF@1-nonanol capsules (1:1) and PSF@1-nonanol capsules (1:3), respectively. Fig. 6 shows the adsorption results, with the increase

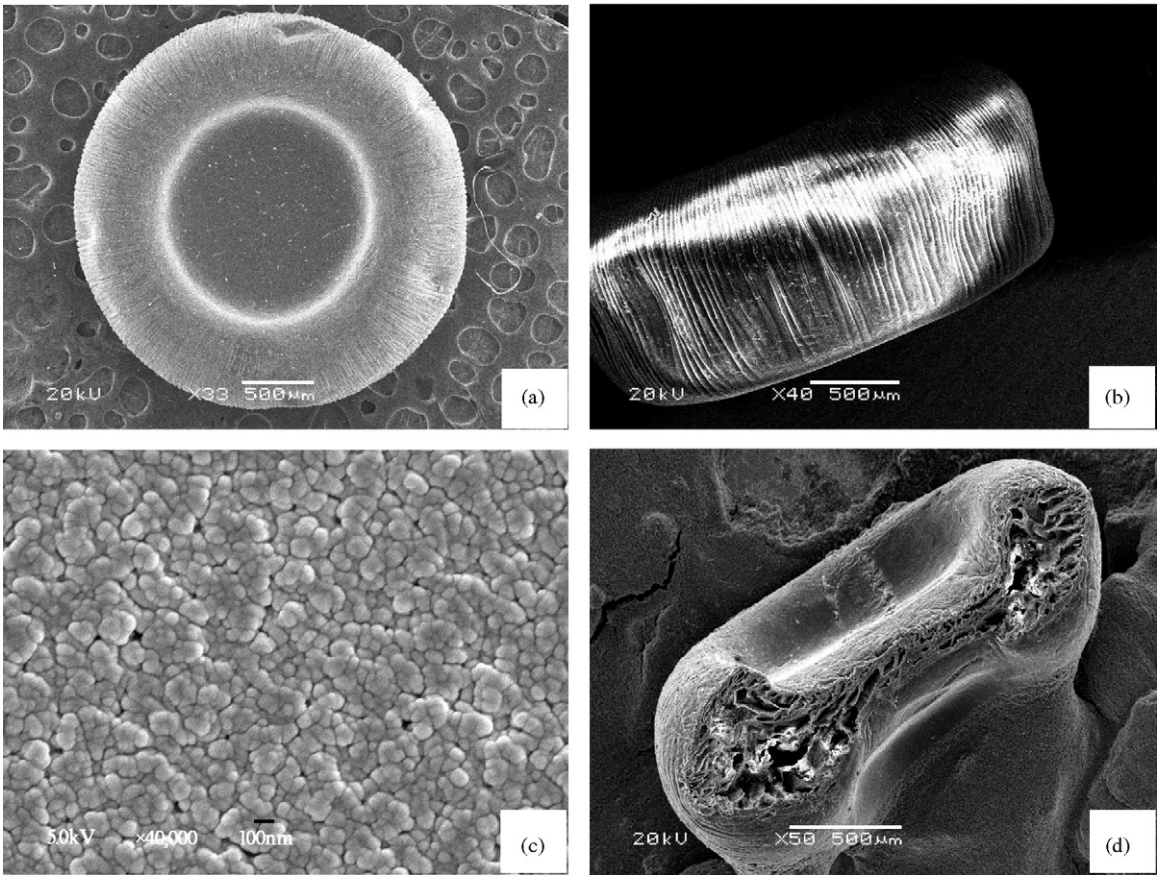

Fig. 3. SEM image of PSF@1-nonanol capsules: (a) facing section, (b) side section, (c) outer surface, (d) cross-section. ((a), (b), and (d) were obtained by SEM, JSM-6380Lv; and (c) was obtained by SEM, JSM-6701F.)

of the 1-nonanol in the capsules, the rate of adsorption increased, whereas the adsorbed phenol amount per unit mass of the capsules decreased. This phenomenon can be explained by further understanding the characters of PSF@1-nonanol capsules used in this study.

According to the results of N_2 adsorption experiment, de-extractant capsules (i.e. PSF) possess of abundant pore structure and great surface area which could provide large numbers of adsorption sites for phenol. Phenol adsorption on de-extractant capsules is driven by van der Waals interaction between the aromatic ring of phenol molecule and the phenyl ring on the matrix of de-extractant capsules (as shown in Fig. 8(a and c)), hydrophobic and hydrogen bonding interaction (as shown in Fig. 8(a and b)). However, in extractant-loaded capsules (i.e. PSF@1-nonanol capsules (1:1) and PSF@1-nonanol capsules (1:3)), the encapsulated 1-nonanol molecules will be further associated with each other to form 1-nonanol clusters (as shown in Fig. 4(a)), which are remarkably stabilized in micropores of PSF@1-nonanol capsules, causing partial blockage of the micropores, reducing the accessible surface area, and impeding or even preventing phenol adsorption onto the

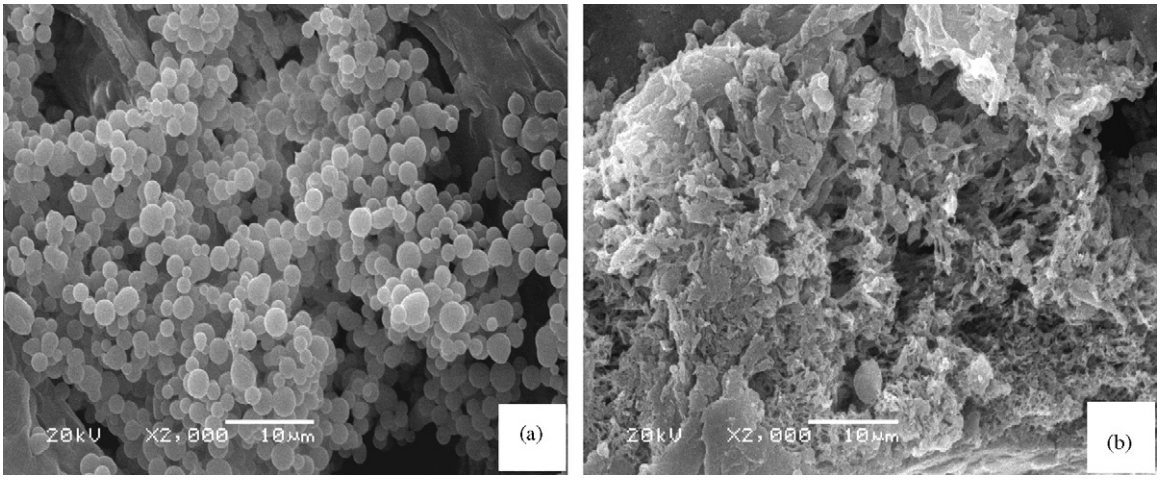

Fig. 4. The SEM images of cross-section of extractant-loaded capsules (a) and de-extractant capsules (b). ((a) and (b) were obtained by SEM, JSM-6380Lv).

Table 1
Summary of surface area and porosity of extractant-loaded capsules and de-extractant capsules.

Capsules	BET surface area (m^2/g)	Volume of pores (cm^3/g)	Average pore width (nm)
Extractant-loaded capsules	4.79	0.009359	903.16
De-extractant capsules	8.49	0.024653	1373.47

matrix of PSF (shell). That is why the adsorbed phenol amount per unit mass of the capsules decreased with the increase of the 1-nonanol in the capsules.

However, the rate of phenol adsorption onto capsules increased with the increase of the 1-nonanol in the capsules. This phenomenon can be explained by further understanding the characters of PSF@1-nonanol capsules and the process of adsorption phenol onto PSF@1-nonanol capsules. In order to further investigate the adsorption capacity contribution and the process of adsorption phenol onto PSF@1-nonanol capsules, 1-nonanol, de-extractant capsules (the prepared method is shown in Section 3.1) and extractant-loaded capsules (i.e. PSF@1-nonanol capsules (1:3)) were used to adsorb phenol, respectively. 4.08 g (the encapsulation capacity of 1-nonanol in 6 g PSF@1-nonanol capsules (1:3)) of 1-nonanol, 1.92 g (the content of PSF in 6 g PSF@1-nonanol capsules (1:3)) of de-extractant capsules and 6 g of PSF@1-nonanol capsules (1:3) were added into each of two 125 mL Erlenmeyer flasks containing 70 mL of phenol solution. As shown in Fig. 7, the rate of adsorption phenol onto 1-nonanol is quite rapid with most of phenol being adsorbed within 1 min. The apparent equilibrium is reached in about 3 min. However, for de-extractant capsules, the adsorption equilibrium of phenol was achieved after 14 h. What is more interesting is the equilibrium time of phenol onto PSF@1-nonanol capsules (1:3) was 1 h which was between 3 min and 14 h. From these results, it is supposed that three consecutive mass transport steps will be associated with the adsorption of phenol from solution by PSF@1-nonanol capsules [6]. First, the phenol rapidly migrates through the solution, i.e. film diffusion, followed by phenol movement from particle surface into interior 1-nonanol clusters by pore diffusion and finally the phenol is adsorbed into the active sites at the interior of PSF (shell) by phenol rapidly migrates through 1-nonanol clusters. 1-nonanol plays a very important role in the first and second step. As we all know, liquid–liquid extraction presents a rapid absorption rate, it is not unexpected that 1-nonanol which is an effective liquid phase extractant to remove phenol from aqueous solution presents a rapid absorption rate. The driving forces of phenol on 1-nonanol are expected to include hydrophobic and hydrogen bonding interaction (as shown in Fig. 8(d)). Therefore, the first and second step takes relatively short contact time, which can be easily comprehended by the foregoing adsorption experiment of phenol onto 1-nonanol. In the second step, phenol movement from particle surface into interior 1-nonanol clusters by pore diffusion, yielding a very high phenol concentration in interior 1-nonanol clusters. The 1-nonanol clusters are remarkably stabilized in the interior pores and interior surface of PSF (shell); hence, the high concentration phenol in 1-nonanol clusters could rapidly diffuse into the active sites at the interior surface of PSF (shell) by the greater driving force by a higher concentration gradient. The three mass transport steps were all very fast, which is the reason that the rate of phenol adsorption onto capsules increased with the increase of the 1-nonanol in the capsules.

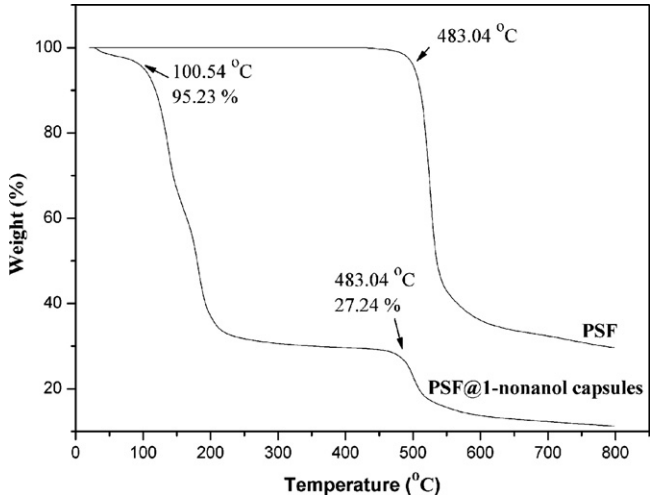

Fig. 5. TGA of the PSF@1-nonanol capsules and PSF (composition of dispersed phase is PSF/1-nonanol/NMP = 8 g/24 g/60 mL; the continuous phase is 0.5 wt.% sodium dodecylbenzenesulfonate).

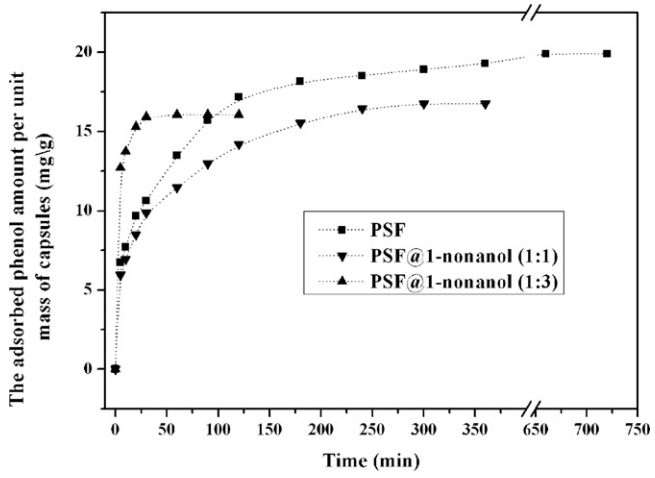

Fig. 6. Effect of contact time and the different mass ratios (PSF to 1-nonanol) on the adsorption phenol amount of capsules from aqueous solutions (C_0: 2048 mg/L, 20 °C, and pH 6).

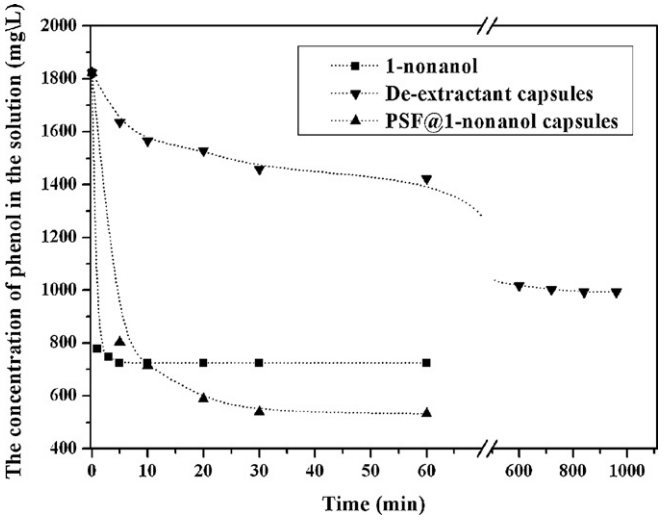

Fig. 7. Adsorption phenol by 1-nonanol, de-extractant capsules and extractant-loaded capsules (C_0: 1822 mg/L, 20 °C, and pH 6).

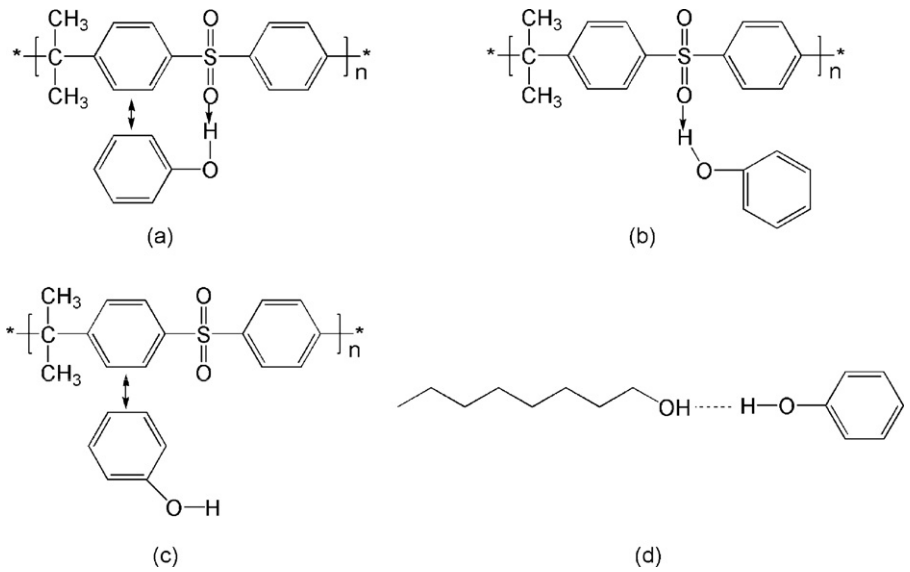

Fig. 8. Schemes for the chemical structure of PSF@1-nonanol capsules and the interactions between PSF@1-nonanol capsules and phenol ((a)–(c) PSF and phenol; (d) 1-nonanol and phenol).

As has been said, the most contribution of 1-nonanol encapsulated in PSF@1-nonanol capsules for phenol adsorption was the enhancement in phenol absorption rate. However, for PSF (shell) in PSF@1-nonanol capsules, the increase in phenol absorption capacity was the most contribution. In order to further investigate the adsorption mechanism of phenol onto PSF@1-nonanol capsules, the sorption behavior and mechanism will be discussed according to the effect of pH, effect of temperature, kinetic and isotherm models in the following section.

3.2.2. Effect of initial phenol concentration

The uptake of phenol, by PSF@1-nonanol capsules, at different values of concentration 993.6, 1908.6, 3133.8, 4089.1, 7003.5 and 9702 mg/L was studied as a function of shaking time by varying the time from 0 to 120 min as presented in Fig. 9. The results show that the rate of adsorption of phenol is initially quite rapid with most of phenol being adsorbed within the first few minutes. The rates of adsorption then slow down with the elapse of time until an apparent equilibrium is reached in about 60–90 min. Moreover, the initial rate of adsorption was greater for higher initial phenol concentration because the resistance to the phenol uptake decreased as the mass transfer driving force increased. The amount of phenol adsorbed at equilibrium per gram of capsules increases from 8.82 to 75.71 mg/g with increase in the initial concentration over the range tested. On the contrary, the removal percentage of phenol from aquatic solution increases from 65.8% to 74.3% as the initial phenol concentration is reduced from 9702 to 993.6 mg/L. These indicate that the initial phenol concentration plays an important role in the adsorption of phenol.

3.2.3. Effect of pH

Solution pH, which primarily affects the degree of ionization of phenol as well as the surface charge of the adsorbents, was one of the most important parameters in controlling the adsorption capacity. Change in pH affects the adsorptive process through dissociation of functional groups of the active sites on the surface of the adsorbent. Therefore, the adsorption of phenol on PSF@1-nonanol capsules was studied at different solution pH between 2 and 12. A Britton–Robinson buffer was employed for pH adjustment: it consists of a mixture of 0.04 M H_3BO_3, 0.04 M H_3PO_4 and 0.04 M CH_3COOH that has been titrated to the desired pH with 0.2 M NaOH. As shown in Fig. 10, it is clear to see that the adsorption capacity

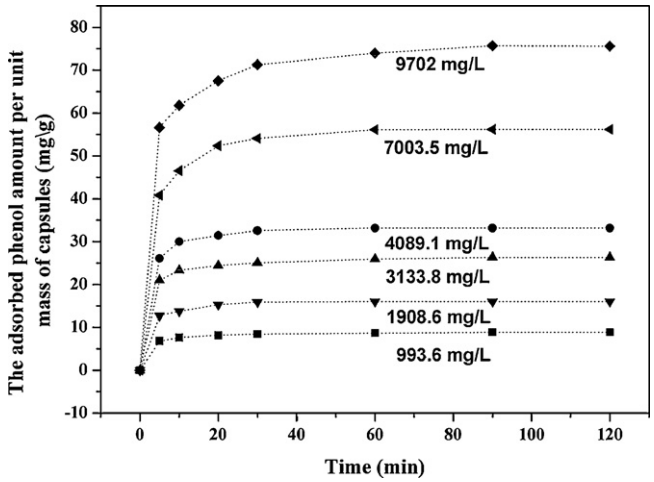

Fig. 9. Effect of contact time and initial phenol concentration on the adsorption phenol amount of PSF@1-nonanol capsules from aqueous solutions (20 °C, pH 6).

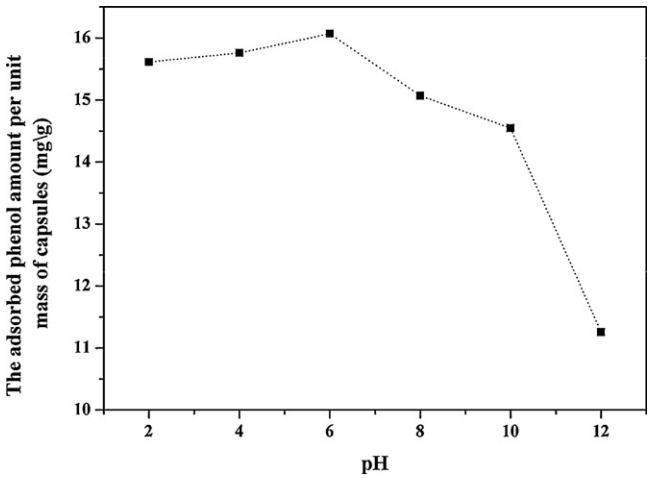

Fig. 10. Effect of solution pH on the adsorption phenol amount of PSF@1-nonanol capsules from aqueous solutions (contact time: 2 h, 20 °C, C_0: 1910 mg/L).

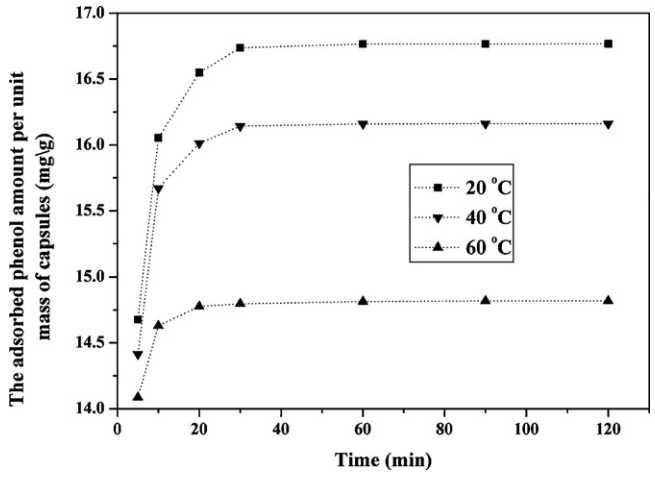

Fig. 11. Effect of contact time and temperature on the adsorption phenol amount of PSF@1-nonanol capsules from aqueous solutions (C_0: 2048 mg/L, pH 6).

slightly increases with increasing pH up to 6 and then decreases with further increasing the pH to alkaline value. The interaction of the phenol molecules with the functional groups on PSF@1-nonanol capsules may follow an extremely complicated pattern. However, the effect of pH on phenol adsorption can be interpreted on the basis of chemical interactions: for solution pH below 6.0, most of the O atoms in the PSF chains are protonated. Hence, a significantly high electrostatic attraction exists between the positively charged surface of PSF@1-nonanol capsules and the phenolate ion, resulting in a great adsorption capacity. The initial pH of the phenol solution is about 6 as phenol was dissolved in neutral water, which is the optimal condition for the phenol adsorption (solution pH below 6.0). That is, the phenol solution which cannot be pH adjusted by hydrochloric acid or sodium hydroxide is the optimal condition for the adsorption. In a basic solution, very few O atoms in the PSF chains and 1-nonanol are protonated, and the electronegative property of O atoms on the PSF chains and 1-nonanol is higher; thus phenol is adsorbed to a lesser extent at higher pH values as the negatively charged surfaces of the adsorbent did not favour the adsorption of phenolate ion due to electrostatic repulsion.

3.2.4. Effect of temperature

The temperature dependence of phenol sorption onto PSF@1-nonanol capsules was studied with the constant initial concentration of 2048 mg/L. Fig. 11 shows the effect of temperature on the sorption of phenol by PSF@1-nonanol capsules as a function of contact time. Interestingly, it was observed that, an increase in temperature results in an increased mobility of phenol molecules, thus the sorption rate slightly increased when the temperature of phenol solution increased from 20 to 60 °C. Conversely, the equilibrium sorption capacity decreased with the temperature rising. This suggests that the process is exothermic indicating that lower temperature is more favourable for the adsorption of phenol. At higher temperatures between 40 and 60 °C, the adsorption was low due to the decrease in physical forces responsible for adsorption or due to the enhancement of thermal energies of PSF@1-nonanol capsules, resulting in the weakening of the attractive force between PSF@1-nonanol capsules and phenol preventing to retain the adsorbed molecules at the active sites [33]. The phenomenon that the equilibrium sorption capacity decreased with the temperature rising could also be further understudied by the intraparticle diffusion model (in the following Section 3.3.1.3). If the adsorption process is controlled by the diffusion process (intraparticle transport-pore diffusion), the sorption capacity will increase with an increase in temperature due to endothermicity of the diffusion process [34].

Table 2
Thermodynamic parameters for the adsorption of phenol on PSF@1-nonanol capsules.

Temperature (K)	K_0	ΔG^0 (kJ mol^{-1})	ΔH^0 (kJ mol^{-1})	ΔS^0 (J mol^{-1} K^{-1})
293	27.4	−8.06	−7.44	2.34
313	24.4	−7.78		
333	19.0	−7.17		

Section 3.3.1.3 showed that intraparticle diffusion is not only rate-limiting mechanism and that some other mechanisms are involved. Therefore, it is reasonable that the equilibrium sorption capacity decreased with the temperature rising.

According to three different temperatures for phenol adsorption (Fig. 11), the thermodynamic parameters standard free energy (ΔG^0), enthalpy change (ΔH^0), and entropy change (ΔS^0) were estimated to evaluate the feasibility and exothermic nature of the adsorption process. The Gibb's free energy change of the process is related to equilibrium constant by the equation:

$$\Delta G^0 = -RT \ \ln K_0 \tag{3}$$

According to thermodynamics, the Gibb's free energy change is also related to the enthalpy change (ΔH^0) and entropy change (ΔS^0) at constant temperature by the following equation:

$$\ln \ K_0 = \frac{\Delta S^0}{R} - \frac{\Delta H^0}{RT} \tag{4}$$

where K_0 ($=Q_e/C_e$) is equilibrium constant. Q_e is the amount of phenol adsorbed by per mass of PSF@1-nonanol capsules (mg/g) and C_e is the phenol concentration in solution at equilibrium (mg/mL). The values of enthalpy change (ΔH^0) and entropy change (ΔS^0) were calculated from the slope and intercept of the plot of $\ln K_0$ versus ($1/T$). These thermodynamic parameters are given in Table 2. The negative ΔG^0 values confirm the feasibility of the adsorption process and the spontaneous nature of adsorption. Negative value of ΔH^0 indicates the exothermic nature of the process. Extent of phenol adsorption decreases because desorption increases with temperature. The positive value of ΔS^0 indicates that there is an increase in the randomness in the system solid/solution interface during the adsorption process.

3.3. Adsorption modeling

3.3.1. Sorption kinetics of phenol

In order to investigate the adsorption mechanism, the pseudo-first-order adsorption, the pseudo-second-order adsorption and the intraparticle diffusion models were used to fit kinetics experimental data. The weighted sample (6 g) of the PSF@1-nonanol capsules was mixed with a 70 mL phenol solution to carry out adsorption studies in a batch mode.

3.3.1.1. The pseudo-first-order kinetic model. The pseudo-first-order kinetic model has been widely used to predict phenol adsorption kinetics. A linear form of pseudo-first-order model was described by Srihari and Das [35].

$$\log(Q_{e1} - Q_t) = \log \ Q_{e1} - \frac{k_1 t}{2.303} \tag{5}$$

where Q_t is the amount of phenol adsorbed (mg/g) on PSF@1-nonanol capsules at various time t, Q_{e1} the maximum adsorption capacity (mg/g) for the pseudo-first-order adsorption, k_1 the pseudo-first-order rate constant for the adsorption process (min^{-1}). The values of $\log(Q_{e1} - Q_t)$ were calculated from the kinetic data. In order to confirm the applicability of the model, the plot of $\log(Q_{e1} - Q_t)$ against t should be a straight line. In a real first-order process, experimental $\log(Q_{e1})$ should be equal to the intercept of

Table 3
The adsorption kinetic model rate constants for phenol on PSF@1-nonanol capsules at different initial phenol concentrations (20 °C, pH 6).

C_0 (mg/L)	Pseudo-first-order			Pseudo-second-order				Intraparticle diffusion		
	Q_{e1} (mg/g)	k_1 (min^{-1})	$R_1{}^2$	Q_{e2} (mg/g)	k_2 (g/mg min)	h (mg g^{-1} min^{-1})	$R_2{}^2$	k_3 (mg/g min$^{1/2}$)	C	$R_3{}^2$
993.6	2.44	0.059	0.9785	8.96	0.0581	4.66	0.9999	3.65	5.91	0.9398
1908.1	7.72	0.1301	0.9767	16.23	0.0491	12.93	0.9999	7.89	10.51	0.9858
3133.8	6.05	0.0546	0.9556	26.67	0.023	16.36	0.9999	9.20	18.89	0.9081
4067.6	14.79	0.1338	0.9387	33.56	0.0285	32.10	0.9999	14.37	22.9	0.8840
7003.5	21.53	0.0795	0.9874	57.14	0.0092	30.04	0.9999	31.90	32.64	0.9547
9702	25.3	0.0575	0.9989	77.52	0.0053	31.85	0.9999	34.83	47.04	0.9933

the straight line. If the intercept dose not equal Q_{e1} then the reaction is not likely to be first-order reaction even this plot has high correlation coefficient with the experimental data [36]. The kinetics data are plotted as the linear form of the models, and the resultant parameters are given in Table 3. It was noticed that the calculated Q_{e1} values are too low compared with experimental Q_e values and the correlation coefficients were also low, ranging from 0.9989 to 0.9387. This shows unsatisfactory applicability of the pseudo-first-order model in predicting the kinetics of phenol adsorption onto the PSF@1-nonanol capsules.

3.3.1.2. The pseudo-second-order kinetic model. The adsorption kinetics can also be described by pseudo-second-order equation:

$$\frac{t}{Q_t} = \frac{1}{k_2 {Q_{e2}}^2} + \frac{t}{Q_{e2}} \quad (6)$$

The second-order rate constants were used to calculate the initial sorption rate (h), given by the following Eq. (7):

$$h = k_2 {Q_{e2}}^2 \quad (7)$$

where Q_t is the amount of phenol adsorbed (mg/g) on PSF@1-nonanol capsules at various time t, Q_{e2} the maximum adsorption capacity (mg/g) for the pseudo-second-order adsorption, k_2 the rate constant of pseudo-second-order for the adsorption (g/mg min).

The linear plots of t/Q_t versus t yielded the second-order rate constant k_2. The Q_{e2} value calculated from the slope of the equation had a good agreement with the experimental Q_e values as seen in Table 3. The values of R^2 and Q_{e2} indicated that this equation produced better results: at all concentrations, R^2 values for pseudo-second-order kinetic model were found to be higher (0.9999), and the calculated Q_e values are mainly equal to the experimental data. Thus, it is inferred that the adsorption system belongs to the pseudo-second-order kinetic model for the entire sorption period. The value of initial sorption (h, mg g^{-1} min^{-1}) that represents the rate of initial sorption, is practically increased with the increase in initial phenol concentrations from 993.6 to 4067.6 mg/L. This could be attributed to the driving force of diffusion. The driving force changes with the phenol concentration in the solution. Thus, the increase of phenol concentration results in an increase in the driving force, which will increase the diffusion rate of the molecular phenol in PSF@1-nonanol capsules. However, the rate of initial sorption almost remains constant with the increase in initial phenol concentrations from 4067.6 to 9702 mg/L. The increase of phenol concentration results in much more sites occupied by phenol in the initial sorption step, but the available amount of the active sites on the surface of PSF@1-nonanol capsules is limited in this step. Therefore, the initial sorption rate (h) will remain constant with the increase in initial phenol concentrations when the active sites were all occupied by phenol in the initial sorption step.

3.3.1.3. The intraparticle diffusion model. Considering that the pseudo-first-order and the pseudo-second-order model could not identify the diffusion mechanism, the intraparticle diffusion model [37] was used. The initial rate of the intraparticle diffusion may be expressed by the following equation:

$$Q_t = k_3 t^{1/2} + C \quad (8)$$

where k_3 is the intraparticle diffusion constant (mg/g min$^{1/2}$), and the value of the intercept C is indicative of the boundary layer. From the plots in Fig. 12, the values of k_3, C and $R_3{}^2$ were calculated and are given along with the correlation factors in Table 3. According to this model, plots of Q_t versus $t^{1/2}$ should be linear and pass through the origin if intraparticle diffusion is the rate controlling step [38]. On the other hand, if the plots are linear but do not pass through the origin the rate of adsorption may be controlled by intraparticle diffusion together with other kinetic models. As shown in Fig. 12, plots of Q_t versus $t^{1/2}$ at different initial concentrations are all linear but they do not pass through the origin. This indicated that intraparticle diffusion is involved in the adsorption process of phenol on the absorbent of PSF@1-nonanol capsules but it is not only rate-limiting mechanism and that some other mechanisms are involved.

3.3.2. Sorption isotherm of phenol

The equilibrium isotherms are very important for understanding the adsorption systems. There are several isotherm equations available for analyzing experimental sorption equilibrium data. The most frequently used for phenols solutions are the Langmuir adsorption isotherm and Freundlich equations. The Langmuir isotherm was developed on the assumption that the adsorption process will only take place at specific homogenous sites within the adsorbent surface with uniform distribution of energy level. Once the adsorbate is attached on the site, no further adsorption can take place at that site; which concluded that the adsorption process is monolayer in nature. Contrarily to Langmuir, Freundlich isotherm was based on the assumption that the adsorption occurs on heterogeneous sites with non-uniform distribution of energy

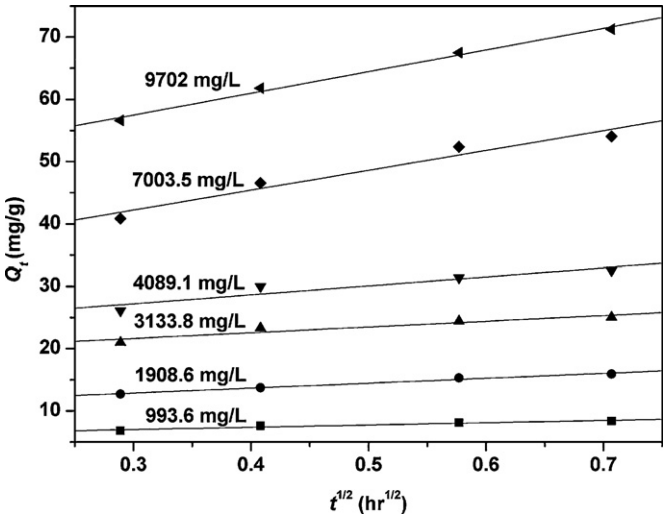

Fig. 12. The fitting of intraparticle diffusion model for phenol on PSF@1-nonanol capsules for different initial concentrations.

Table 4
The Langmuir and Freundlich equations, the values of parameters and correlation coefficients (20 °C, pH 6).

Langmuir			Freundlich		
Q_m (mg/g)	K_L (L/mg)	R^2	K (mg/g) (L/mg)$^{1/n}$	n	R^2
250	0.00013	0.89	0.076	1.17	0.999

level. The Freundlich describes reversible adsorption and is not restricted to the formation of monolayer [8]. The linear form of Langmuir and Freundlich equations are represented by Eqs. (9) and (10), respectively.

$$\text{Langmuir equation}: \quad \frac{C_e}{Q_e} = \frac{1}{K_L Q_{\max}} + \frac{C_e}{Q_{\max}} \tag{9}$$

$$\text{Freundlich equation}: \quad \ln Q_e = \ln K + \frac{1}{n} \ln C_e \tag{10}$$

where C_e (mg/L) is the concentration of the phenol solution at equilibrium, Q_e (mg/g) is the amount of sorption at equilibrium. In Langmuir equation, $Q_{\max}$ is the maximum sorption capacity and K_L is Langmuir constant. These constants can be evaluated from the intercept and the slope of the linear plot of experimental data of C_e/Q_e versus C_e, respectively. In Freundlich equation, K and $1/n$ are empirical constants. These constants can be evaluated from the intercept and the slope of the linear plot of $\ln Q_e$ versus $\ln C_e$. The R^2 values shown in Table 4 are evident that the phenol adsorption in this study is well fitted Freundlich model compared with Langmuir model; it can deduce that phenol was adsorbed on heterogeneous sites with non-uniform distribution of energy level in PSF@1-nonanol capsules [8]. This phenomenon can be further explained by understanding the characters of PSF@1-nonanol capsules used in this study. The capsules were synthesized by phase inversion (immersion) precipitation technique, using PSF as a shell material and 1-nonanol as the core. Both PSF and 1-nonanol play important roles in the adsorption process. However, PSF is solid material and 1-nonanol is liquid, which may cause differences in the energy level of the active sites available on PSF@1-nonanol capsules thus affecting its adsorption power.

The Langmuir and Freundlich equations, values of parameters and correlation coefficients of the experimental data are shown in Table 4. From Table 4, we can conclude as follows: (i) the Langmuir maximum capacity was found to be 250 mg/g, but the correlation coefficient R is so low that the calculated results may be not credible. (ii) The slope $1/n$, ranging between 0 and 1 is indicative of the relative energy distribution on the adsorbent surface (or surface heterogeneity) [39]. (iii) The Freundlich correlation coefficient is higher than the Langmuir correlation coefficient. It indicates that the Freundlich isotherm shows better fit to adsorption than the Langmuir isotherm.

3.4. Regeneration of the capsules

The effect of regeneration on adsorption capacity of phenol onto the PSF@1-nonanol capsules from aqueous solutions was studied using batch and column experiments. In batch adsorption–regeneration cycles, the adsorption capacity of phenol onto the PSF@1-nonanol capsules every time was calculated and the results are plotted in Fig. 13. Adsorption–regeneration cycles were then performed seven times but no further decrease of adsorption capacity could be measured. Multiple column adsorption–regeneration cycles of PSF@1-nonanol capsules were also performed to further test its potential application. No further decrease of adsorption capacity (Fig. 14) indicated that PSF@1-nonanol capsules can be effectively regenerated for repeated use.

SEM and TGA were employed to investigate the characters of PSF@1-nonanol capsules after seven times of repeated extraction and stripping. The results of SEM and TGA in batch and column experiments were almost analogical, so we only showed the SEM and TGA of PSF@1-nonanol capsules in batch experiments. Fig. 15 shows SEM images of cross-section of PSF@1-nonanol capsules after seven times of repeated extraction and stripping. There are a lot of small particles with a diameter of several microns in the wall of the regenerated capsules, which were the same with fresh capsules (Fig. 4(a)). In order to observe the encapsulation capacity of PSF@1-nonanol capsules after seven times of repeated extraction and stripping, TGA of regenerated capsules was carried out. Fig. 16 shows the TGA result, the encapsulation capacity of capsules as calculated was 59.68%, which was slightly lower than the fresh PSF@1-nonanol capsules. These experiments show that the PSF@1-nonanol capsules could be reused without significant loss of their initial properties.

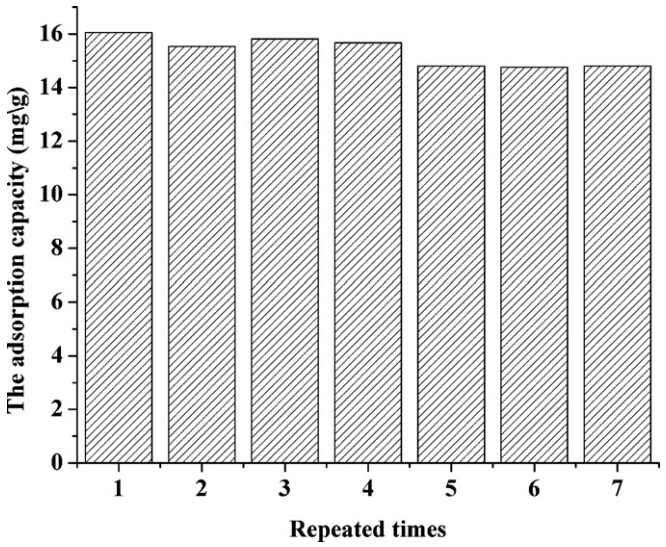

Fig. 13. Effect of regeneration on the adsorption capacity of phenol onto PSF@1-nonanol capsules from aqueous solutions using batch experiments (contact time: 2 h, 20 °C, C_0: 1852.3 mg/L).

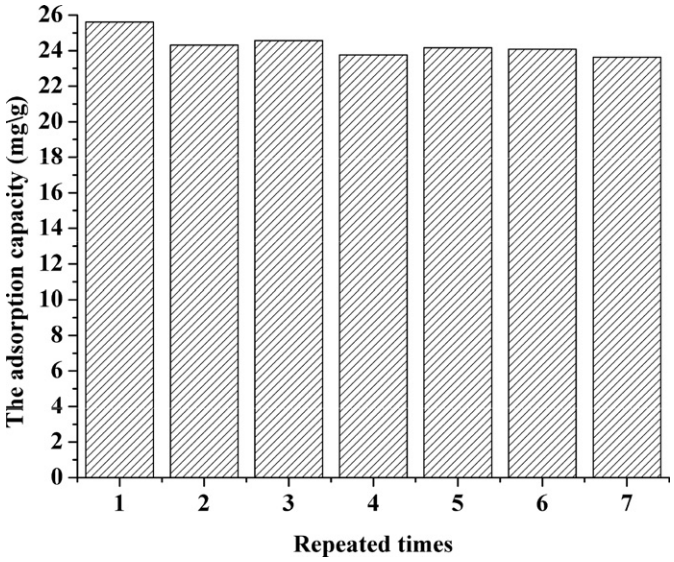

Fig. 14. Effect of regeneration on the adsorption capacity of phenol onto PSF@1-nonanol capsules from aqueous solutions using column experiments (velocity: 1.0 mL/min, 20 °C, C_0: 1822 mg/L).

Table 5
Comparison of various adsorbents for the adsorption of phenol from aqueous solutions.

Adsorbent	Initial phenol concentration	pH	T (°C)	Equilibrium time	Capacity[a] (mg/g)	Refs
Activated carbon						
Biomass material	~200 mg/L	–	~30	~1200 min	149.25	[6]
Commercial	~100 mg/L	–	~20	~60 min	49.72	[7]
Coconut shell	~500 mg/L	~7.0	~30	~2880 min	205.842	[8]
Natural materials						
Montmorillonite	~300 mg/L	~10.2	~25	~200 min	20.8	[9]
Kaolin	~300 mg/L	~10.2	~25	~250 min	7.8	[9]
OMMT-PSF capsule	~4000 mg/L	~7.0	~30	~360 min	97.18	[10]
Bioadsorbents						
Modified green macro alga	~150 mg/L	~5.9	~30	~300 min	24.86	[11]
Chitin	~100 mg/L	~1.0	~25	~100 min	24.15	[12]
Chicken feathers	~100 mg/L	–	~25	~2880 min	19.46	[13]
Waste materials						
Beet pulp	~100 mg/L	~6.0	~25	~100 min	89.96	[14]
Neutralized red mud	~200 mg/L	~6.0	~25	~600 min	4.127	[15]
Bagasse fly ash	~200 mg/L	~6.5	~30	~300 min	23.832	[16]
Polymeric resin						
PVBPE	~400 mg/L	~6.0	~15	~700 min	55.56	[2]
MCH-111	~200 mg/L	–	~30	~720 min	97.34	[40]
CHA-111	~200 mg/L	–	~30	~720 min	95.52	[40]
XAD-7	~800 mg/L	~7.0	~25	~30 min	78.7	[41]
Solvent capsule						
PSF@1-nonanol capsules	~993.6 mg/L	~6.0	~20	~60 min	250	Present work
	~7003.5 mg/L	~6.0	~20	~60 min		
	~9702 mg/L	~6.0	~20	~90 min		

[a] The maximum uptake capacity estimated from the Langmuir model.

3.5. Comparison of various adsorbents for phenol removal

A comparison of sorption capacity of PSF@1-nonanol capsules with conventional adsorbents was presented in Table 5. It was noticed that most of them focus on the adsorption of low concentration phenol (less than 1000 mg/L), and the rates of adsorption of phenol were all quite slow. We can infer, for phenol solutions with higher initial concentrations, longer equilibrium times were required by conventional adsorbents, thus adding extra operational costs for waste treatment. However, as compared to conventional adsorbents, PSF@1-nonanol capsules display the best kinetic performance and adsorption capacity for high concentration phenol adsorption. Furthermore, taken into account the fact that the exhausted PSF@1-nonanol capsules are easy to an entire regeneration for repeated use, PSF@1-nonanol capsules can be taken as an ideal adsorbent for rapid removal of high concentration phenol from aqueous solution.

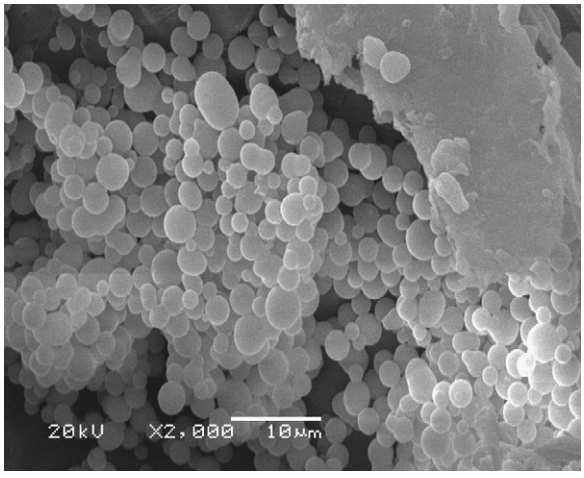

Fig. 15. The SEM images of cross-section of PSF@1-nonanol capsules after seven times of repeated extraction and stripping.

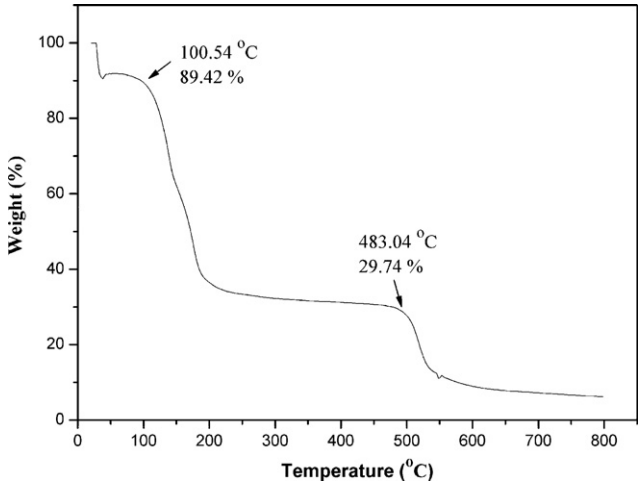

Fig. 16. The TGA of PSF@1-nonanol capsules after seven times of repeated extraction and stripping.

4. Conclusions

In this study, a novel kind of solvent capsules with biconcave disc-shaped and rugate characteristics, i.e. PSF@1-nonanol capsules, was successfully prepared by using a phase inversion (immersion) precipitation technique. The characters and sorption behavior of PSF@1-nonanol capsules were investigated, and the following results were obtained:

(1) Its characteristic biconcave disc-shaped and rugate morphology benefits mass transfer performance.
(2) Phenol adsorption uptake was found to increase with increase in initial concentration and adsorption time, whereas

adsorption of phenol was more favourable at acidic pH and low temperature.
(3) The adsorption kinetics of phenol by PSF@1-nonanol capsules followed pseudo-second-order model. The results of sorption isotherm showed that the Freundlich isotherm shows a better fit to adsorption than the Langmuir isotherm.
(4) The rate of adsorption of phenol is initially quite rapid and equilibrium is reached in about 90 min.
(5) The PSF@1-nonanol capsules have very good stability in the adsorption process.

The results showed that PSF@1-nonanol capsules were a promising alternative adsorbent for rapidly removing phenol from aqueous solutions at a high concentration. The PSF@1-nonanol capsules are also expected to be used as a rapid adsorbent for other organic pollution. Besides, the PSF@1-nonanol capsules are promising to use in the broad technical areas of a two-phase partitioning bioreactor (capsules could be used as the partitioning phase) and high performance liquid chromatography (capsules could be used to concentrate of trace target compounds).

Acknowledgments

The authors thank the financial supports from the Committee of Natural Science Foundation in China on National Training Fund for Person with Ability of Basic Subjects (J0730425) and Key Research Program of Gansu Province (2GS064-A52-036-02).

References

[1] M. Ahmaruzzaman, Adsorption of phenolic compounds on low-cost adsorbents: a review, Adv. Colloid Interface 143 (2008) 48–67.
[2] J.H. Huang, K.L. Huang, A.T. Wang, Q. Yang, Adsorption characteristics of poly(styrene-co-divinylbenzene) resin functionalized with methoxy and phenoxy groups for phenol, J. Colloid Interface Sci. 327 (2008) 302–307.
[3] A. Knop, L.A. Pilato, Phenolic Resins—Chemistry, Applications and Performance, Springer-Verlag, 1985.
[4] U.S. Environmental Protection Agency, National Recommended Water Quality Criteria–Correction, EPA 822-Z-99-001, Washington, DC, 1999.
[5] A. Krishnaiah, Adsorption of phenol and p-chlorophenol from their single and bisolute aqueous solutions on Amberlite XAD-16 resin, J. Hazard. Mater. 105 (2003) 143–156.
[6] B.H. Hameed, A.A. Rahman, Removal of phenol from aqueous solutions by adsorption onto activated carbon prepared from biomass material, J. Hazard. Mater. 160 (2008) 576–581.
[7] B. Özkaya, Adsorption and desorption of phenol on activated carbon and a comparison of isotherm models, J. Hazard. Mater. 129 (2006) 158–163.
[8] A.T. Mohd Din, B.H. Hameed, A.L. Ahmad, Batch adsorption of phenol onto physiochemical-activated coconut shell, J. Hazard. Mater. 161 (2009) 1522–1529.
[9] S.H. Lin, R.C. Hsiao, R.S. Juang, Removal of soluble organics from water by a hybrid process of clay adsorption and membrane filtration, J. Hazard. Mater. 135 (2006) 134–140.
[10] G. Zhao, L. Zhou, Y. Li, X. Liu, Enhancement of phenol degradation using immobilized microorganisms and organic modified montmorillonite in a two-phase partitioning bioreactor, J. Hazard. Mater. (2009), doi:10.1016/j.jhazmat.2009.03.110.
[11] R. Aravindhan, J.R. Rao, B.U. Nair, Application of a chemically modified green macro alga as a biosorbent for phenol removal, J. Environ. Manage. 90 (2009) 1877–1883.
[12] A.Y. Dursun, C.D. Kalayci, Equilibrium, kinetic and thermodynamic studies on the adsorption of phenol onto chitin, J. Hazard. Mater. 123 (2005) 151–157.
[13] F.A. Banat, S. Al-Asheh, Biosorption of phenol by chicken feathers, Environ. Eng. Policy 2 (2000) 85–90.
[14] G. Dursun, H. Cicek, A.Y. Dursun, Adsorption of phenol from aqueous solution by using carbonised beet, J. Hazard. Mater. 125 (2005) 175–182.
[15] A. Tor, Y. Cengeloglu, M.E. Aydin, M. Ersoz, Removal of phenol from aqueous phase by using neutralized red mud, J. Colloid Interface Sci. 300 (2006) 498–503.
[16] V.C. Srivastava, M.M. Swamy, I.D. Mall, B. Prasad, I.M. Mishra, Adsorptive removal of phenol by bagasse fly ash and activated carbon: equilibrium, kinetics and thermodynamics, Colloids Surf. A 272 (2006) 89–104.
[17] H.S. Gao, J.M. Xing, X.C. Xiong, Immobilization of ionic liquid [BMIM][PF6] by spraying suspension dispersion method, Ind. Eng. Chem. Res. 47 (2008) 4414–4417.
[18] X.C. Gong, G.S. Luo, W.W. Yang, F.Y. Wu, Separation of organic acids by newly developed polysulfone microcapsules containing triotylamine, Sep. Purif. Technol. 48 (2006) 235–243.
[19] W.W. Yang, G.S. Luo, F.Y. Wu, F. Chen, X.C. Gong, Di-2-ethylhexyl phosphoric acid immobilization with polysulfone microcapsules, React. Funct. Polym. 61 (2004) 91–99.
[20] W.W. Yang, G.S. Luo, X.C. Gong, Extraction and separation of metal ions by a column packed with polystyrene microcapsules containing aliquat 336, Sep. Purif. Technol. 43 (2005) 175–182.
[21] W.W. Yang, G.S. Luo, X.C. Gong, Polystyrene microcapsules containing aliquat 336 as a novel packing material for separation of metal ions, Hydrometallurgy 80 (2005) 179–185.
[22] K. Kondo, E. Kamio, Separation of rare earth metals with a polymeric microcapsule membrane, Desalination 144 (2002) 249–254.
[23] S. Nishihama, N. Sakaguchi, T. Hirai, I. Komasawa, Extraction and separation of rare earth metals using microcapsules containing bis(2-ethylhexyl)phosphinic acid, Hydrometallurgy 64 (2002) 35–42.
[24] Z.Y. Xiang, Y.C. Lu, Y. Zou, X.C. Gong, G.S. Luo, Preparation of microcapsules containing ionic liquids with a new solvent extraction system, React. Funct. Polym. 68 (2008) 1260–1265.
[25] C.O. Illanes, N.A. Ochoa, J. Marchese, Kinetic sorption of Cr(VI) into solvent impregnated porous microspheres, Chem. Eng. J. 136 (2008) 92–98.
[26] A. Laguecir, B. Ernst, Y. Frere, L. Danicher, M. Burgard, Extraction of metal cations by polyterephthalamide microcapsules containing a poly(acrylic acid) gel, J. Microencapsul. 19 (2002) 17–28.
[27] A. Laguecir, Y. Frere, L. Danicher, M. Burgard, Size effect of complexing microcapsules on copper ion extraction, Eur. Polym. J. 38 (2002) 977–981.
[28] T. Saito, S. Torii, Microcapsule for adsorption and recovery of cadmium (II) ion, Sep. Sci. Technol. 37 (2002) 77–87.
[29] W.W. Yang, Y.C. Lu, Z.Y. Xiang, G.S. Luo, Monodispersed microcapsules enclosing ionic liquid of 1-butyl-3-methylimidazolium hexafluorophosphate, React. Funct. Polym. 67 (2007) 81–86.
[30] L.D. Collins, A.J. Daugulis, Biodegradation of phenol at high initial concentrations in two-phase partitioning batch and fed-batch bioreactors, Biotechnol. Bioeng. 55 (1997) 155–162.
[31] R.D. Yang, A.E. Humphrey, Dynamic and steady state studies of phenol biodegradation in pure and mixed cultures, Biotechnol. Bioeng. 17 (1975) 1211–1235.
[32] I.M. Wienk, R.M. Boomm, M.A.M. Beerlage, A.M.W. Bulte, C.A. Smolders, H. Strathmann, Recent advances in the formation of phase inversion membranes made from amorphous or semi-crystalline polymers, J. Membr. Sci. 113 (1996) 361–371.
[33] D.N. Jadhav, A.K. Vanjara, Removal of phenol from wastewater using sawdust, polymerized saw dust and saw dust carbon, Indian J. Chem. Technol. 11 (2004) 35–41.
[34] V.C. Srivastava, I.D. Mall, I.M. Mishra, Adsorption thermodynamics and isosteric heat of adsorption of toxic metal ions onto bagasse fly ash (BFA) and rice husk ash (RHA), Chem. Eng. J. 132 (1–3) (2007) 267–278.
[35] V. Srihari, A. Das, The kinetic and thermodynamic studies of phenol-sorption onto three agro-based carbons, Desalination 225 (2008) 220–234.
[36] G. Crini, H.N. Peindy, F. Gimbert, C. Robert, Removal of C.I. Basic Green 4 (Malachite Green) from aqueous solutions by adsorption using cyclodextrin based adsorbent: kinetic and equilibrium studies, Sep. Purif. Technol. 53 (2007) 97–110.
[37] W.J. Weber Jr., J.C. Morris, Kinetics of adsorption on carbon from solution, J. Sanit. Eng. Div. Proceed. Am. Soc. Civil Eng. 89 (1963) 31–59.
[38] S. Mitali, A.P. Kumar, B. Bhaskar, Modeling the adsorption kinetics of some priority organic pollutants in water from diffusion and activated energy parameters, J. Colloid Interface Sci. 206 (2003) 28–32.
[39] W.T. Tsai, Y.M. Chang, C.W. Lai, C.C. Lo, Adsorption of basic dyes in aqueous solution by clay adsorbent from regenerated bleaching earth, Appl. Clay Sci. 29 (2005) 149–154.
[40] B.C. Pan, Y. Xiong, A.M. Li, J.L. Chen, Q.X. Zhang, X.Y. Jin, Adsorption of aromatic acids on an aminated hypercrosslinked macroporous polymer, React. Funct. Polym. 53 (2002) 63–72.
[41] B.J. Pan, B.C. Pan, W.M. Zhang, Q.R. Zhang, Q.X. Zhang, S.R. Zheng, Adsorptive removal of phenol from aqueous phase by using a porous acrylic ester polymer, J. Hazard. Mater. 157 (2008) 293–299.